

# Study of Indirect Vector Control Induction Motor Based on Takagi Sugeno Type Fuzzy Logic on Rotational Speed Control Primary Surveillance Radar

Paulus Setiawan, Muchamad Wizdan Dharmawan, Prasidananto Nur Santoso, Elisabeth Anna Pratiwi, Okto Dinaryanto

Institut Teknologi Dirgantara Adisutjipto, Lanud Adisutjipto Jl. Janti Blok R, Yogyakarta 55198, Indonesia

## ARTICLE INFO

### Article history:

Received April 15, 2024

Revised June 24, 2024

Published July 26, 2024

### Keywords:

Induction motor;  
Takagi Sugeno;  
Fuzzy logic;  
Indirect vector control

## ABSTRACT

During the rainy season and bad weather, strong winds blowing at an airport can cause dynamic changes in performance of the primary surveillance radar (PSR) antenna which is driven by an induction motor (IM). Changes in dynamic performance that occur in this IM can be in the form of changes in PSR rotation speed, changes in torque values, and changes in stator current values. In this article, we propose the application of the Takagi Sugeno method to fuzzy logic indirect vector control of IM as a solution that can reduce changes in the dynamic performance of motor as PSR drivers during bad weather. The contribution of this research is the application of the Takagi Sugeno method in a fuzzy inference system (FIS), where this fuzzy logic control system replaces the conventional proportional integral (PI) controller for indirect vector control IM. Takagi Sugeno method is computationally efficient and works well with optimization and adaptive techniques, which makes it very attractive in control problems, particularly for dynamic nonlinear systems. Takagi Sugeno type FIS uses weighted average to compute the crisp output, so the Sugeno's output membership functions are either linear or constant. Furthermore, Takagi Sugeno method has better processing time since the weighted average replace the time consuming defuzzification process. The results obtained after simulation in MATLAB Simulink environment showed that fuzzy logic using the Takagi Sugeno method which is used as a substitute controller for indirect vector control can provide better performance when compared to conventional PI controllers. These results can be seen from the response values of rotor rotation speed, electromagnetic torque, and stator current. Overall, this research provides discourse on improving the dynamic performance of IM through the application of the Takagi Sugeno fuzzy logic indirect vector control method.

This work is licensed under [aCreative Commons Attribution-Share Alike 4.0](https://creativecommons.org/licenses/by-sa/4.0/)



## Corresponding Author:

Paulus Setiawan, Institut Teknologi Dirgantara Adisutjipto, Lanud Adisutjipto Jl. Janti Blok R, Yogyakarta 55198, Indonesia

Email: [paulussetiawan@itda.ac.id](mailto:paulussetiawan@itda.ac.id)

## 1. INTRODUCTION

Induction motor (IM) is a type of electric motor that works based on electromagnetic induction. IM has a source of electrical energy, namely on the stator side, while the electrical system on the rotor side is induced through the air gap from the stator with electromagnetic media, so this is what can cause the motor to be named an induction motor. The use of IM in industry is as a driver for blowers, compressors, pumps, main drivers of production processes or mills, and so on. In this research, IM is used as a driver for primary surveillance radar (PSR) and the problem in this research is that during the rainy season and bad weather, the wind will blow strongly at an airport Fig. 1. For the record, if the wind is categorized as a strong wind, then the wind is moving at a speed of more than 20 knots [1]. Wind moving at high speeds can cause dynamic changes in performance

of the IM-driven PSR antenna. Changes in dynamic performance that occur in this IM can include changes in the oscillation response in the system to become slower in reaching the settling time value, so that this situation results in a decrease in the PSR rotation speed, an increase in the electromagnetic torque value, and an increase in the current value in the stator. To prevent changes in dynamic performance that are quite large, it is necessary to have a controller on IM with a certain method so that changes in dynamic performance that occur are smaller than using the previous controller.

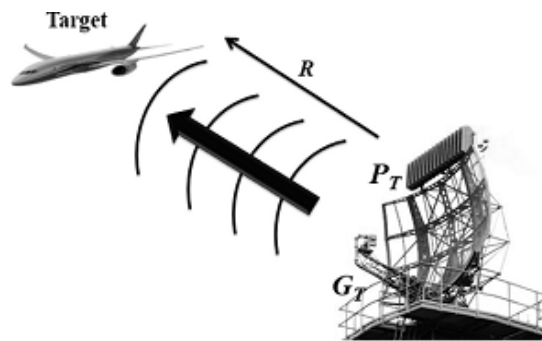


Fig. 1. Primary Surveillance Radar (PSR) [2]

Research using the fuzzy logic method for controlling induction motors has been carried out by [3]. In this research, the fuzzy logic block used as an IM controller is a replacement for the field oriented control (FOC) block. The results of this research are that fuzzy logic which is used as a replacement FOC controller can provide high dynamic performance such as faster transient response as a result of faster computing time when compared to conventional FOC controllers. Then research using the quantum lightning search algorithm (QLSA) method for optimizing the rotational speed control of IM has been developed and implemented in fuzzy logic controllers to produce fuzzy membership function inputs so that in the process of computing fuzzy rules can produce outputs that are suitable for controlling IM [4], [5].

Designing and implementing a self tuning fuzzy logic controller (ST-FLC) in indirect field oriented control (IFOC) in IM speed controller can provide better performance when compared to conventional proportional integral (PI) controllers [6], [7]. By using nine rules in the fuzzy logic computing process, ST-FLC provides good performance in steady and transient conditions which can be seen in the results of response overshoot, rise time, settling time and recovery time. Then research that analyzed the comparison of the use of fuzzy rules with the numbers 9, 25, and 49, gave performance results that with fewer rules or simplified to 5, 7, and 9, speed control on IM was better [8]-[10].

Previous research related to the application of fuzzy logic methods in vector control such as an extended Kalman filter (EKF) algorithm for the estimation of rotor speed of a squirrel cage IM from the measured line currents [11]. Based on combination of the fuzzy logic approach and sensorless approach the all in real time experience, fuzzy logic was used for the robustness regardless of the accuracy of the motors model, with the use of Luenberger estimator for the motor's speed estimation [12]. Use of offline fuzzy tuned PID controller for a space vector pulse width modulation (SVPWM) fed indirect field oriented control (IFOC) of IM drive [13]. Presentation simulation results obtained from a feedforward vector controlled IM drive under varying operating conditions like step change in speed command and step change in torque command [14]. In these studies [8]-[14], the method used as rules in fuzzy logic is the Mamdani method.

Research that has comparatively analyzed the application of the Mamdani and Takagi Sugeno fuzzy inference system (FIS) in the calibration of continuous time car follower models by proposing a methodology that allows parallel data processing and determination of the simulation model output resulting from the application of both fuzzy techniques was carried out by [15]. In this study, the Takagi Sugeno FIS provides more accurate compensation values, resulting in behavior that is more similar to the observed model. Then the same research comparing the Mamdani and Sugeno methods on control systems with the addition of proportional integral derivative (PID) compensators has been carried out by [16]-[18]. The results of this research are that the Sugeno inference model is very suitable for nonlinear systems, which can be linearized in finding solutions to control systems. It can be said that the advantages of the theory and application of the Sugeno inference method include computational efficiency which can work well with linear techniques as a substitute for PID control, has high compatibility with optimization and adaptive techniques, and guarantees the continuity of the output surface and the suitability of mathematical analysis.

The novelty that will be presented in this research is the analysis of IM testing which is used as a primary surveillance radar (PSR) driver with a fuzzy logic indirect vector control using the Takagi Sugeno method. Then the IM performance response results with the fuzzy controller are compared with the scalar controller and conventional PI controller. The fuzzy logic indirect vector control in IM is basically a controller that replaces the PI controller. The test analysis was carried out starting when there was no load and testing when it was under load where there were very strong gusts of wind. Then the response results that will be analyzed are the response to changes in rotor speed, stator current response, and electromagnetic torque response. The contribution of this research is the application of the Takagi Sugeno method in a fuzzy inference system (FIS), where this fuzzy logic control system replaces the conventional proportional integral (PI) controller for indirect vector control IM. The Sugeno inference model is very suitable for nonlinear systems, which can be linearized in finding solutions to control systems.

## 2. METHODS

In this research, a fuzzy logic indirect vector control simulation will be carried out on IM using the Takagi Sugeno method with Matlab simulink, where fuzzy logic indirect vector control can be used as a solution to reduce the response to changes in the dynamic performance of the motor as a PSR driver during bad weather. The first step taken is to model the IM, where the motor parameter values [19] are in Appendix B, into dynamic equations. The aim of IM dynamic modeling is to be able to determine the stator current value, electromagnetic torque value, and other IM parameter values. After dynamic modeling, the second step is to design an IM controller with a scalar controller, where in this scalar controller the method used is the PWM method. Then the third step is to design indirect vector control on IM with a conventional PI controller. And the fourth or final step is to design fuzzy logic indirect vector control on IM, where this fuzzy logic uses the Takagi Sugeno method with 3 (three) Gaussian membership functions and functions as a replacement for the conventional PI controller.

### 2.1. Induction Motor and Dynamic Modelling

Induction motor control is broadly divided into two methods, namely scalar control and vector control. Scalar control as the basis of control is to maintain the voltage value divided by the frequency value, so that if the voltage value increases then the frequency value must also be increased [20]-[26]. By only controlling the constant ratio of voltage and frequency values, controlling motor rotation speed using the scalar control method is a simple method and is widely applied in industries but will provide a slow transient response. This is what causes the scalar control method to be less suitable when applied to motors that serve loads whose characteristics are dynamic [27]. The methods that can be written as a sequence in building indirect vector control are as follows.

Dynamic modeling of IM is the modeling of voltage, current and torque equations that describe the dynamic behavior of IM which vary with time. These equations can be used to solve differential equations where there is some complexity [19]. Changes in variables may occur and to reduce the problem of complexity of these equations can be achieved by eliminating all inductance parameters that change with time, due to the nature of the electric circuit which moves relatively from the motor voltage equations. The equivalent circuit in the voltage and flux equations for an induction motor is shown in Fig. 2. For the equation of voltage and sound flux in terminology or inductive reactance terms it can be written as

$$v_{qs} = r_s i_{qs} + \frac{\omega}{\omega_b} \psi_{ds} + \frac{p}{\omega_b} \psi_{qs} \quad (1)$$

$$v_{ds} = r_s i_{ds} + \frac{\omega}{\omega_b} \psi_{qs} + \frac{p}{\omega_b} \psi_{ds} \quad (2)$$

$$v_{0s} = r_s i_{0s} + \frac{p}{\omega_b} \psi_{0s} \quad (3)$$

$$v'_{qr} = r'_r i'_{qr} + \left( \frac{\omega - \omega_r}{\omega_b} \right) \psi'_{dr} + \frac{p}{\omega_b} \psi'_{qr} \quad (4)$$

$$v'_{dr} = r'_r i'_{dr} + \left( \frac{\omega - \omega_r}{\omega_b} \right) \psi'_{qr} + \frac{p}{\omega_b} \psi'_{dr} \quad (5)$$

$$v'_{0r} = r'_r i'_{0r} + \frac{p}{\omega_b} \psi'_{0r} \quad (6)$$

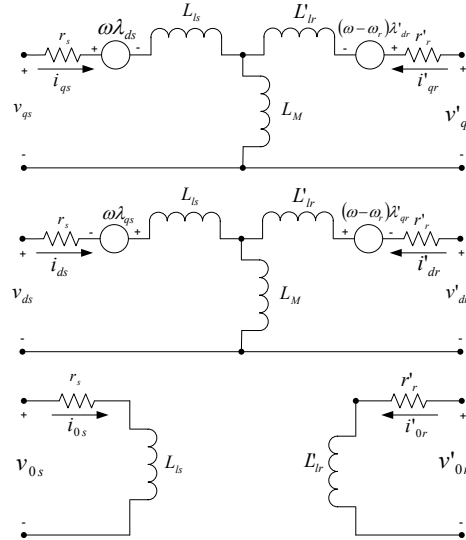


Fig. 2. Arbitrary reference frame equivalent circuits for a 3 phase, symmetrical IM [19]

From equations (1)-(6), where  $\omega_b$  is the electrical angular velocity used to compute the inductive reactance value. So then the scope flux equation in voltage units per second becomes

$$\psi_{qs} = X_{ls} i_{qs} + X_M (i_{qs} + i'_{qr}) \quad (7)$$

$$\psi_{ds} = X_{ls} i_{ds} + X_M (i_{ds} + i'_{dr}) \quad (8)$$

$$\psi_{0s} = X_{ls} i_{0s} \quad (9)$$

$$\psi'_{qr} = X'_{lr} i'_{qr} + X_M (i_{qs} + i'_{qr}) \quad (10)$$

$$\psi'_{dr} = X'_{lr} i'_{dr} + X_M (i_{ds} + i'_{dr}) \quad (11)$$

$$\psi'_{0r} = X'_{lr} i'_{0r} \quad (12)$$

From equations (7)-(12), then the equation to simulate a symmetric induction motor with an arbitrary reference frame can be created by first solving the scope flux equation or the flux per second equation for current so that it can be written as

$$i_{qs} = \frac{1}{X_{ls}} (\psi_{qs} - \psi_{mq}) \quad (13)$$

$$i_{ds} = \frac{1}{X_{ls}} (\psi_{ds} - \psi_{md}) \quad (14)$$

$$i_{0s} = \frac{1}{X_{ls}} \psi_{0s} \quad (15)$$

$$i'_{qr} = \frac{1}{X'_{lr}} (\psi'_{qr} - \psi_{mq}) \quad (16)$$

$$i'_{dr} = \frac{1}{X'_{lr}} (\psi'_{dr} - \psi_{md}) \quad (17)$$

$$i'_{or} = \frac{1}{X'_{lr}} \psi'_{or} \tag{18}$$

From equations (13)-(18), where  $\psi_{mq}$  and  $\psi_{md}$ , which are useful when representing saturation, are defined as

$$\psi_{mq} = X_M(i_{qs} + i'_{qr}) \tag{19}$$

$$\psi_{md} = X_M(i_{ds} + i'_{dr}) \tag{20}$$

With this dynamic modeling approach (19), (20) a three-phase winding can be reduced to a two-phase ( $d$ - $q$ ) winding with a magnetic axis winding formed on the quadrature axis. In other words, the stator variables and rotor variables (such as voltage, current and flux linkages) of an IM are transferred into the reference frame, can rotate at any angular speed or remain stationary in Fig. 3. Such a reference frame is generally known in IM analysis as an arbitrary reference frame.

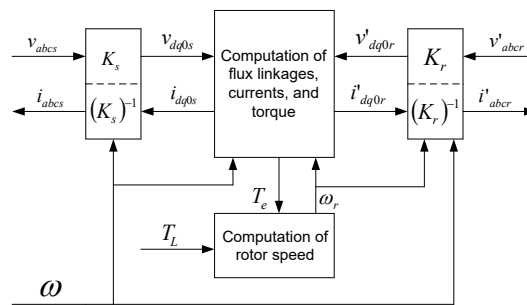


Fig. 3. Block diagram of a symmetrical 3 phase induction machine in the arbitrary reference frame [19]

**2.2. Transformation abc-dq0**

The transformation of a 3 phase circuit into a 2 phase reference frame was developed by E. Clarke, where the 2 phase reference frame is the  $\alpha$  axis and the  $\beta$  axis. Then, so that the transformation of the 2 phase reference frame can be reversed in the calculation, a third variable can be added as a component of the zero sequence. So the resulting transformation is  $[f_{\alpha\beta 0}] = T_{\alpha\beta 0}[f_{abc}]$ , where  $f$  represents voltage, current, flux linkages, and as a transformation matrix of  $T_{\alpha\beta 0}$  is [28].

$$T_{\alpha\beta 0} = \frac{2}{3} \begin{bmatrix} 1 & -\frac{1}{2} & -\frac{1}{2} \\ 0 & \frac{\sqrt{3}}{2} & -\frac{\sqrt{3}}{2} \\ \frac{1}{2} & \frac{1}{2} & \frac{1}{2} \end{bmatrix} \tag{21}$$

Then R.H. Park introduced a new approach to the analysis of electrical machines. Park formulated changes in variables that replace variables such as voltage, current, and flux linkages associated with fictitious windings that rotate on the rotor. Park refers the stator and rotor variables to a reference frame mounted on the rotor. From the rotor's point of view, all these variables can be observed as constant values. So the resulting transformation is in the form  $[f_{dq0}] = T_{dq0}[f_{abc}]$ , where  $f$  also represents voltage, current, flux linkages, and as a transformation matrix of  $T_{dq0}$  is

$$T_{dq0s}(\theta) = \frac{2}{3} \begin{bmatrix} \cos(\theta) & \cos\left(\theta - \frac{2\pi}{3}\right) & \cos\left(\theta + \frac{2\pi}{3}\right) \\ \sin(\theta) & \sin\left(\theta - \frac{2\pi}{3}\right) & \sin\left(\theta + \frac{2\pi}{3}\right) \\ \frac{1}{2} & \frac{1}{2} & \frac{1}{2} \end{bmatrix} \tag{22}$$

### 2.3. Pulse Width Modulation (PWM)

Pulse width modulation (PWM) provides a way to decrease the total harmonic distortion of load current. A PWM inverter output, with some filtering, can generally meet THD requirements more easily than the square wave switching scheme. The unfiltered PWM output will have a relatively high THD, but the harmonics will be at much higher frequencies than for a square wave, making filtering easier. Control of the switches for sinusoidal PWM output requires a reference signal, sometimes called a modulating or control signal, which is a sinusoid in this case and a carrier signal, which is a triangular wave that controls the switching frequency [29]. Suboscillation method employs individual modulators in each of the three phases (Fig. 4(a)). Exemplified waveforms for phase  $a$  are shown in Fig. 4(b), consisting of the sinusoidal reference voltage  $u^*_a$  and the triangular carrier signal  $u_c$  of frequency  $f_s$ . The switched output waveform is  $u'_a$ . The maximum value of the modulation index,  $m_{max1} = \frac{\pi}{4} = 0.785$  is reached at a point where the amplitudes of the reference and the carrier signal become equal Fig. 4(b) [30].

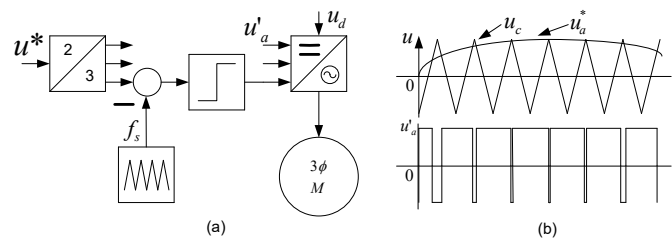


Fig. 4. Suboscillation method. (a) Signal flow diagram. (b) Waveforms, phase a [30]

### 2.4. Speed Controller

A proportional-plus-integral (PI) controller is used to process the speed error between the speed reference and filtered speed feedback signals. The transfer function of the speed controller is given as equation

$$G_s(s) = \frac{K_s(1 + sT_1)}{sT_s} \quad (23)$$

where are the gain and time constants of the speed controller, respectively [31]. Speed control design using this method has also been used in research on permanent magnet synchronous motors used in hydraulic pump systems [32].

### 2.5. Vector Control

Vector control is broadly divided into two methods, namely direct vector control (DTC) and indirect vector control or better known as field oriented control (FOC). In the DTC controller [33]-[38], the motor rotation speed control system is determined by directly regulating the electromagnetic torque and linkage flux. The electromagnetic torque and linkage flux settings are determined through voltage and frequency settings, where the voltage and frequency values on the induction motor are determined by the inverter output value. The inverter output value is determined by the inverter modulation pulses which activate the switches of the inverter. Then the inverter modulation pulses in the DTC motor control method are determined from the calculated error values between the reference torque and the feedback torque and the reference flux values and the feedback flux.

### 2.6. Indirect Vector Control

In the FOC controller Fig. 5, the motor rotation speed control system is determined by indirectly regulating electromagnetic torque and linkage flux. The electromagnetic torque and linkage flux settings are determined by setting the stator current in the direct ( $d$ ) and quadrature ( $q$ ) axes [39]-[53]. The  $d$ -axis current ( $i_d$ ) represents the linkage flux component and the  $q$ -axis current ( $i_q$ ) represents the electromagnetic torque component. The electromagnetic torque reference is determined by a proportional integral (PI) controller, where the PI controller is determined by the comparison between the motor rotation speed reference and the motor rotation speed feedback. With the constant torque angle concept, the  $d$ -axis current ( $i_d$ ) for the linkage flux component is equal to zero ( $i_d = 0$ ). The  $q$ -axis current ( $i_q$ ) and  $d$ -axis current ( $i_d$ ) that have been obtained are then converted into a three-phase  $abc$  axis using the Clark and Park inversion transformation. After obtaining the three-phase reference current  $abc$ , using the pulse width modulation (PWM) method, the ignition pulses of the three-phase inverter can be determined.

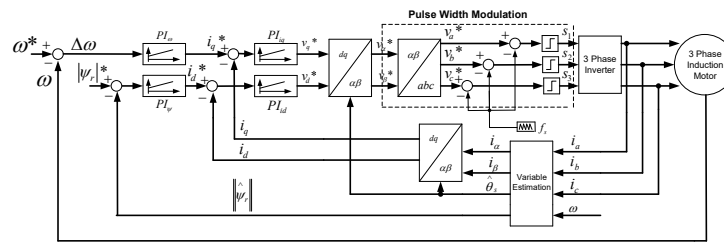


Fig. 5. Indirect Vector Control [40]

The difference between the DTC method and the FOC method is that the DTC method uses switching tables, while the FOC method uses the PWM method. The advantage of the FOC method compared to the DTC method is that the electromagnetic torque response and rotational speed response of the induction motor are better. Meanwhile, the disadvantage of the FOC method when compared to the DTC method is that the FOC method requires a more complex calculation algorithm. The advantage of the FOC method compared to the scalar control method is that it can control current with a fast response so that the FOC method is suitable when applied to motors that serve loads with dynamic characteristics.

2.7. Takagi Sugeno Fuzzy Logic Controller

Reasoning using the Sugeno method is almost the same as Mamdani reasoning, only the output (consequence) of the system is not in the form of a fuzzy set, but in the form of a constant or linear equation. Takagi Sugeno proposed the use of singletons as membership functions of consequents [54]-[57]. A singleton is a fuzzy set with a membership function that at a certain point has a value and 0 outside that point. There are 2 Fuzzy models of the Sugeno method, namely as follows:

- a. Zero Order Fuzzy Sugeno Model  
In general, the zero order Fuzzy Sugeno model is: If  $(x_1 \text{ is } A_1) \bullet (x_2 \text{ is } A_2) \bullet (x_3 \text{ is } A_3) \bullet \dots \bullet (x_n \text{ is } A_n)$  Then  $z = k$  with  $A_i$  is the  $i$ -th fuzzy set as the antecedent, and  $k$  is a constant as the consequent.
- b. First Order Fuzzy Sugeno Model  
In general, the form of the First Order Fuzzy Sugeno model is: If  $(x_1 \text{ is } A_1) \bullet (x_2 \text{ is } A_2) \bullet (x_3 \text{ is } A_3) \bullet \dots \bullet (x_n \text{ is } A_n)$  Then  $z = p_1 \times x_1 + \dots + p_n \times x_n + q$  with  $A_i$  is the  $i$ -th fuzzy set as an antecedent, and  $p_i$  is an  $i$ -th constant and  $q$  is also a constant in the consequent.
- c. The input of the defuzzification process is a fuzzy set resulting from the composition process and the output is a value. For the fuzzy If Then rule in the equation  $RU(k) = \text{If } x_1 \text{ is } A_{1k} \text{ and } \dots \text{ and } x_n \text{ is } A_{nk}$  Then  $y \text{ is } B_k$ , where  $A_{1k}$  and  $B_k$  respectively are fuzzy sets in  $U_1R$  ( $U$  and  $V$  are physical domains),  $i = 1, 2, \dots, n$  and  $x = (x_1, x_2, \dots, x_n)U$  and  $y \in V$  respectively are the input and output (linguistic) variables of the fuzzy system. The defuzzification method is carried out by calculating the Weight Average (WA):

$$WA = \frac{\alpha_1 z_1 + \alpha_2 z_2 + \alpha_3 z_3 + \dots + \alpha_n z_n}{\alpha_1 + \alpha_2 + \alpha_3 + \dots + \alpha_n} \tag{24}$$

where  $WA$  = average value,  $\alpha_n$  = predicate value of the  $n$ -th rule and  $z_n$  = index of the  $n$ -th output value (constant).

The rule reasoning process is a determination of the defuzzification method for each solution variable. At this defuzzification stage, the values of a variable will be selected as in Fig. 6 and Table 1, which will then be analyzed so that the result is the output of the fuzzy area. The method used in this research is the Takagi Sugeno method, where in this method we can approach the analysis in linear equations.

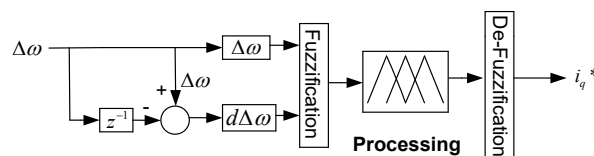


Fig. 6. Fuzzy logic control Model

In Table 1, we take nine pieces of data for each data, and . These nine data are fuzzy reasoning with three gaussian membership functions, so there are also nine rules required. The explanation can be seen in Appendix A. The preparation of fuzzy rules that connect input quantities and controller outputs is connected by the AND operator, which means finding the minimum value of the input membership function. Then we will get the

minimum value of the results and the output membership function as shown in Fig. 7. And the overall method in this research is in the flowchart in Fig. 8.

**Table 1.** Data resulting from simulation processing in fuzzy logic indirect vector control

No.	$\Delta\omega$	$d\Delta\omega$	$i_q^*$
1	314	314	1143.9
2	313.91	-0.0087	1347.4
3	266.3	-0.0844	2309.8
4	262.56	-0.0743	2892.5
5	216.8	-0.0467	3639.2
6	200.02	-0.1525	4133.2
7	135.05	-0.13	4877.4
8	-0.825	-0.00014	5209.5
9	0.485	-0.00059	5213.4

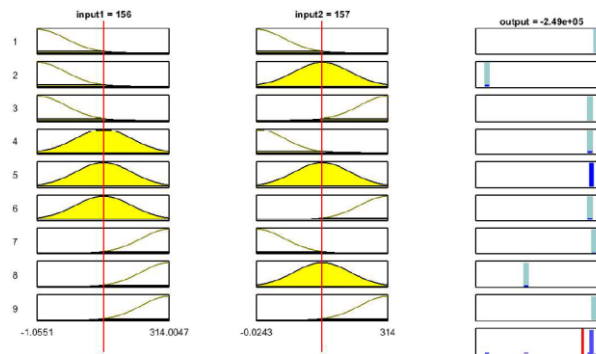


**Fig. 7.** Membership functions fuzzy logic controller

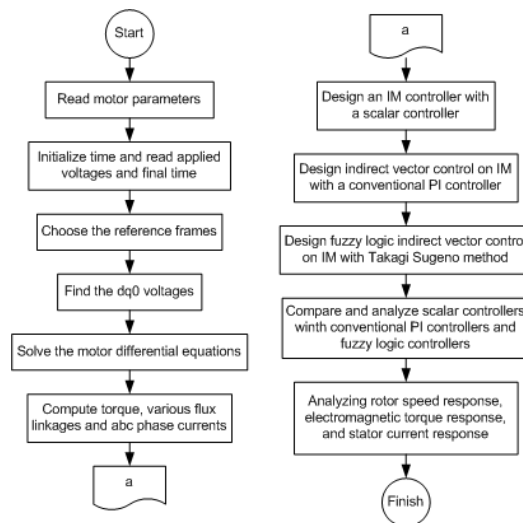


**Fig. 8.** Research system flowchart

### 3. RESULTS AND DISCUSSION

In this research, a fuzzy logic indirect vector control simulation will be carried out on IM using the Takagi Sugeno method with Matlab simulink, where fuzzy logic indirect vector control can be used as a solution to reduce the response to changes in the dynamic performance of the motor as a PSR driver during bad weather (Fig. 9).

#### 3.1. Rotor speed response of the IM in state 1, state 2, and state 3

The simulation model of the rotor speed response characteristics of an IM is shown in Fig. 10. The characteristic that can be seen in this figure is that there is a time comparison between the three controllers which can be calculated from the rise time value and the settling time value. In the initial state when the IM

rotates without load until it reaches a steady state value of rotor speed of 1421 Rpm, the IM with a scalar controller has a rise time value of 0.16 second. Then for IM with PI controllers they have a rise time value of 0.137 second and IM with fuzzy logic controllers have a rise time value of 0.122 second. This comparison shows that the IM with a fuzzy logic controller has a rise time value of 12.29% faster than the PI controller and 31.48% faster than the scalar controller. The characteristics of the settling time value for IM with scalar controllers, PI controllers and fuzzy logic controllers are 0.24 second, 0.2 second and 0.18 second respectively. The characteristics of this settling time value show that an IM with a fuzzy logic controller has 11.11% faster time compared to a PI controller and 33.33% faster than a scalar controller. The results of this research are that fuzzy logic which is used as a replacement controller for FOC can provide high dynamic performance such as faster transient response as a result of faster computing time when compared to conventional FOC controllers, which is comparable to research conducted by [3].

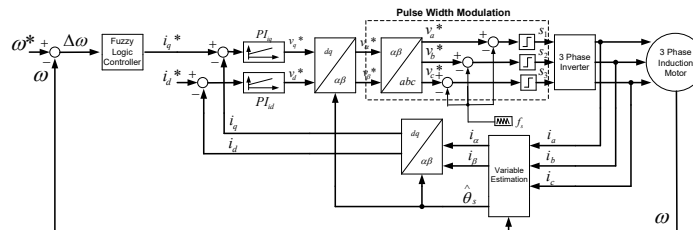


Fig. 9. Fuzzy logic indirect vector control

Then in the second situation, this situation describes the scenario of disturbances originating from strong gusts of wind of 350Nm, the decrease that occurs in the IM with a scalar controller, PI controller, and fuzzy logic controller respectively is 1317 Rpm, 1382 Rpm, and 1393 Rpm. This also shows that the IM with a fuzzy logic controller is able to withstand a decrease in rotor speed of 1.97% to the steady state value of rotor speed of 1421 Rpm. The reduction value that occurs in an IM with a fuzzy logic controller of 1,97% is the smallest reduction value when compared to the value of the reduction in rotor speed with a PI controller and a scalar controller, whose values are 2.74% and 7.32% respectively.

In the third condition (Fig. 11) where the wind gust scenario is reduced by 150Nm, the rotor speed of the IM increases. The characteristics of the increase in rotor rotation speed until it reaches steady state can be seen from the settling time value. The settling time values for the scalar controller, PI controller, and fuzzy logic controller are 0.94 second, 0.9 second, and 0.88 second respectively. From the results of the settling time assessment, it indicates that the rotor speed response with the fuzzy controller is 2.27% faster than the PI controller and 6.82% faster than the scalar controller.

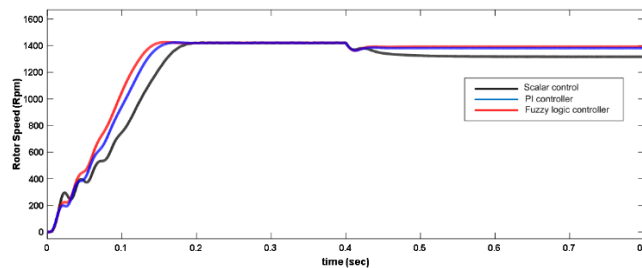


Fig. 10. Speed performance comparison of IM at state 1 and state 2

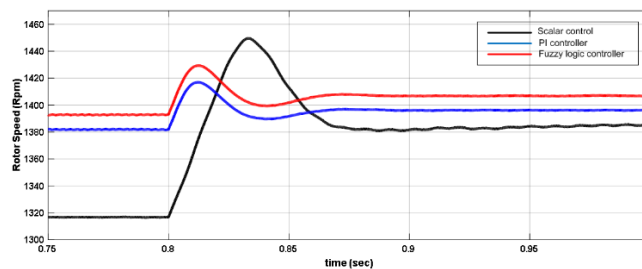


Fig. 11. Speed performance comparison of IM at state 3

### 3.2. Electromagnetic torque response of the IM in state 1, state 2, and state 3

In Fig. 12 shows an analysis of the electromagnetic torque response characteristics of an induction motor with a scalar controller, PI controller and fuzzy logic controller. In the figure, the electromagnetic torque response increases until it reaches a maximum value and then decreases until it reaches a steady state. In the first situation when starting an induction motor with a fuzzy logic controller, the electromagnetic torque response has a maximum value of 958 Nm with a time span of 0.013 seconds and then decreases to a value of 0.26 Nm to reach a steady state with a time of 0.22 seconds. The maximum torque value of an induction motor with a fuzzy logic controller, namely 958 Nm, is 1.69% higher than the maximum torque value of an induction motor with a PI controller, which is 942 Nm. Meanwhile, the steady state time value with a fuzzy logic controller of 0.22 seconds is 7,27% faster than the steady state time value for a system using a PI controller with a time of 0.18 seconds. This faster steady state time value is related to the computing time of the system. The control system in this research uses three Gaussian membership functions with nine rules so that the resulting computing time is faster. As one of the conclusions of this research, it is comparable to research conducted by [8], where in this research the method used was comparing computing time with several number of membership functions and the number of rules used.

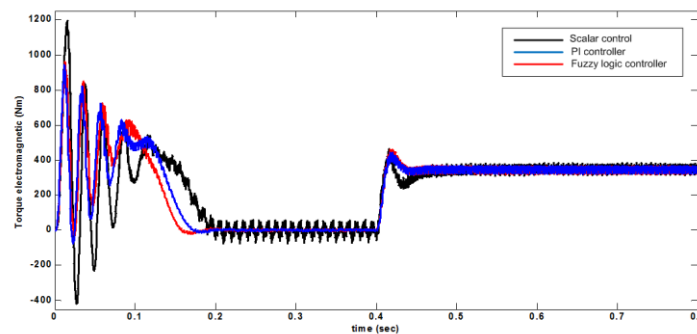


Fig. 12. Electromagnetic torque ( $T_e$ ) performance comparison of IM at state 1 and state 2

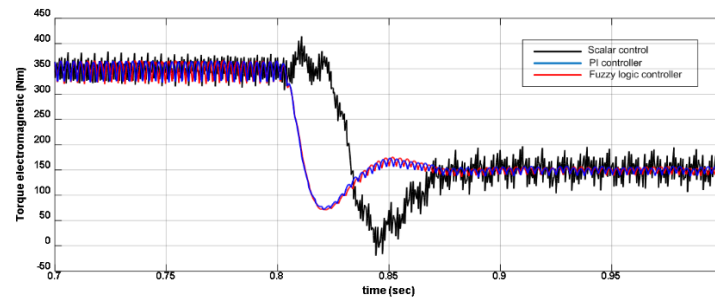


Fig. 13. Electromagnetic torque ( $T_e$ ) performance comparison of IM at state 3

Then in the second situation, when there is an increase in load due to strong wind gusts equivalent to 350 Nm, there appears to be a slight difference in the electromagnetic torque characteristics, a system with a fuzzy logic controller experiences an increase faster than a system with a PI controller. In the first, second, and third conditions as found in Fig. 12 and Fig. 13, the oscillations that occur in the system with the fuzzy logic controller are smaller compared to the oscillations that occur in the system with the scalar controller. So, if this is applied in real situations, an induction motor with a scalar controller will have noisy operations in its working operation which is caused by quite large oscillations in the rotor.

### 3.3. Stator current response of the IM in state 1, state 2, and state 3

In Fig. 14 shows the stator current characteristics of an induction motor from initial starting to steady state conditions. At the time of initial starting, the three stator currents reach a maximum value of 183.4 Amperes with a time span of 0.135 seconds to reach steady state with a value of 8.3 Amperes. The maximum stator current value with a fuzzy logic controller of 183,4 Ampere is 11.8% lower than the maximum stator current value with a PI controller which is 164.1 Ampere. Meanwhile, the steady state time value with a fuzzy logic controller, namely 0.135 seconds, is 25% faster than the steady state time value with a fuzzy logic

controller with a time of 0.18 seconds. In the steady state condition, each stator current obtained is 36 Amperes with a scalar controller, 23.4 Amperes with a PI controller, and 22.2 Amperes with a fuzzy logic controller. So if the results of this calculation are used as a comparison in percentage units, it is with the fuzzy logic controller that the stator current is recorded at 38.3% lower than the scalar controller and 5.13% lower than the PI controller.

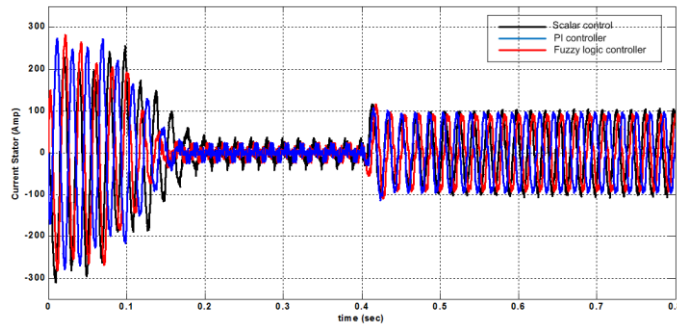


Fig. 14. Stator current ( $i_a$ ) performance comparison of IM at state 1 and state 2

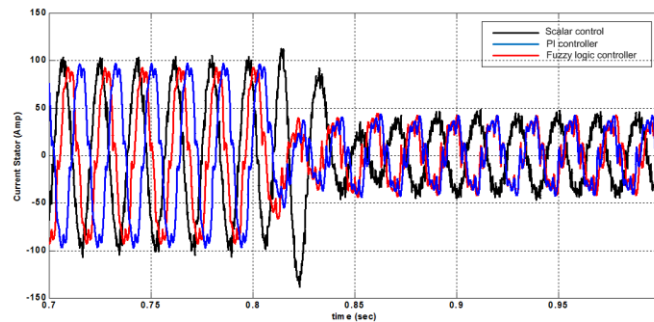


Fig. 15. Stator current ( $i_a$ ) performance comparison of IM at state 3

In Fig. 14 which shows when there is an increase in load due to strong wind gusts and in Fig. 15 when there is a decrease in wind gusts, both only show a slight difference in the characteristics of the stator current between the system with the fuzzy logic controller and the system using the PI controller. When there is an increase in wind gusts which is equivalent to an additional load of 350 Nm, the system that uses a fuzzy logic controller has a stator current value which was initially steady state at 7.2 Ampere, increasing to 19.3 Ampere in 1.54 seconds. Meanwhile, the system that uses a PI controller has a stator current value that was initially steady state at a value of 7.2 Amperes, increasing to 21.2 Amperes. So the system that uses a fuzzy logic controller has a stator current value of 9.9% lower than the system that uses a PI controller. This lower current value shows that the fuzzy logic indirect vector control on the IM has a lower heat value, so this lower heat value will result in more efficient consumption of electrical power. And with the Takagi Sugeno inference method, it has the advantage of computational efficiency which can work well for nonlinear systems [16]. As a correlation to the stator current, the total harmonic distortion (THD) is directly proportional to the stator current where the fuzzy logic controller has the lowest THD value, namely 15.67% (Fig. 17) compared to the scalar controller and the controller which are respectively equal to 24.96% and 21.97% (Fig. 16).

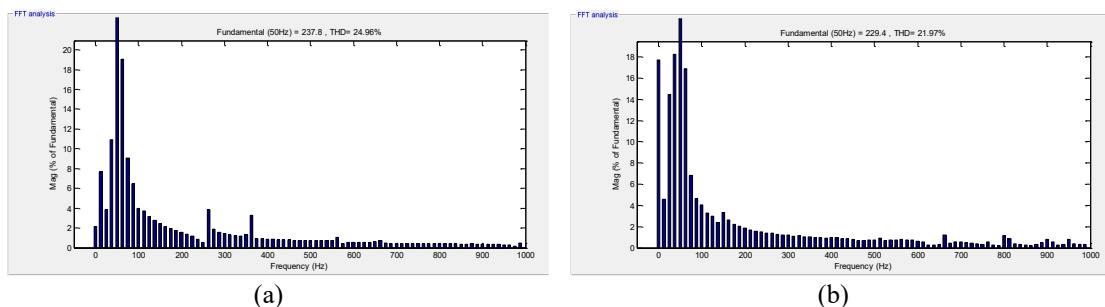


Fig. 16. Total Harmonic Distortion (THD) in (a) scalar controller, (b) PI controller

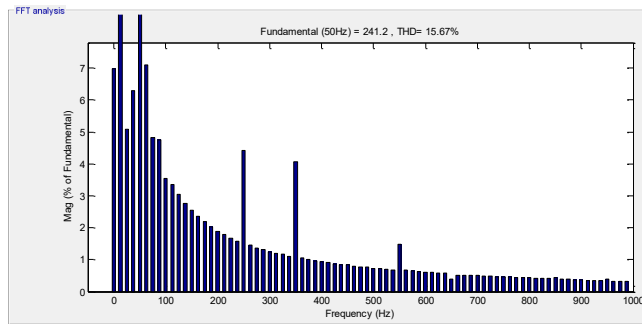


Fig. 17. Total Harmonic Distorsion (THD) in fuzzy logic controller

#### 4. CONCLUSION

Based on this research, the results have been obtained that when strong gusts of wind occur, the IM with a scalar controller experiences a speed decrease of 104 Rpm from the initial steady state value. To overcome this problem, the fuzzy logic indirect vector control methodology in IM using the Takagi Sugeno method is used to reduce the oscillation response faster and it can reduce the decrease in rotor rotation speed when strong wind gusts occur. In this research, the results also showed that the dynamic response of the fuzzy controller was faster when compared to the conventional PI controller. With the Takagi Sugeno inference method, it has the advantage of computational efficiency which can work well for nonlinear systems, so it can be used as a method in optimization systems. From some of the results of the discussion previously explained, it can be concluded that the proposed controller, namely fuzzy logic indirect vector control on IM with the Takagi Sugeno method, can significantly reduce the system oscillation response to be 6.82% faster when compared to the scalar controller, and can reduce the decrease the rotor rotation speed when strong gusts of wind occurs is 1.97% of the IM steady state speed of 1421 Rpm. Future research efforts may be to develop artificial neural networks, where this artificial neural network is to optimize fuzzy logic computing using the Takagi Sugeno method.

#### Acknowledgements

The author would like to thank the Adisutjipto Institute of Aerospace Technology (ITD Adisutjipto) for funding this internal research so that this research can be completed with good and smooth results.

#### APPENDIX. A

In Table 1, we take nine pieces of data for each data  $\Delta\omega$ ,  $d\Delta\omega$ , and  $i_q^*$ . These nine data are fuzzy reasoning with three membership functions, so there are also nine rules required. The explanation is as follows:

##### 1. Data point $\Delta\omega = 314$ , $d\Delta\omega = 314$ , and $i_q^* = 1143.9$

###### 1.1. Making fuzzy sets and inputs

There are 2 fuzzy variables that will be modeled, namely:

- $\Delta\omega$  consists of 3 fuzzy sets, namely N (Negative), Z (Zero), and P (Positive).
- $d\Delta\omega$  consists of 3 fuzzy sets, namely N (Negative), Z (Zero), and P (Positive).

###### A. Variable $\Delta\omega$

To represent  $\Delta\omega$  variables, a Gaussian curve is used, a membership function:

$$f(x, \sigma, c) = e^{-\frac{(x-c)^2}{2\sigma^2}}. \text{ For } \mu_{wN} \sigma = 53.49; \text{ and } c = -0.8247; \mu_{wZ} \sigma = 53.49; \text{ and } c = 156.6; \text{ and } \mu_{wP} \sigma = 53.49; \text{ and } c = 314.$$

If  $\Delta\omega = 314$  then the fuzzy membership value in each set is:

$$\text{Fuzzy set N, } \mu_{wN} [314] = 0.0000028; \text{ Z, } \mu_{wZ} [314] = 0.6034; \text{ and } \mu_{wP} [314] = 1$$

###### B. Variabel $d\Delta\omega$

To represent  $d\Delta\omega$  variables, a Gaussian curve is used, a membership function:

$$f(x, \sigma, c) = e^{-\frac{(x-c)^2}{2\sigma^2}}. \text{ For } \mu_{dwN} \sigma = 53.39; \text{ and } c = -0.2413; \mu_{dwZ} \sigma = 53.39; \text{ and } c = 156.9; \text{ and } \mu_{dWP} \sigma = 53.39; \text{ and } c = 314.$$

If  $d\Delta\omega = 0.00001679$  then the fuzzy membership value in each set is:

Fuzzy set N,  $\mu_{wN}$  [314] = 0.0000030; Z,  $\mu_{wZ}$  [314] = 0.6057; and P,  $\mu_{wP}$  [314] = 1

### 1.2. Fuzzy operator application

**First rule;** [R1] if  $\Delta\omega$  is N and  $d\Delta\omega$  is N then  $i_q^* = x_1$ ; the operator used is AND, then:

$$\alpha_1 = \mu_{predikatR1} = \min(\mu_{wN} [314], \mu_{dwN} [314]) = (0.0000028; 0.0000030) = 0.0000028$$

**Second rule;** [R2] if  $\Delta\omega$  is N and  $d\Delta\omega$  is Z then  $i_q^* = x_2$ ; the operator used is AND, then:

$$\alpha_2 = \mu_{predikatR2} = \min(\mu_{wN} [314], \mu_{dwZ} [314]) = (0.0000028; 0.6057) = 0.0000028$$

**Third rule;** [R3] if  $\Delta\omega$  is N and  $d\Delta\omega$  is P then  $i_q^* = x_3$ ; the operator used is AND, then:

$$\alpha_3 = \mu_{predikatR3} = \min(\mu_{wN} [314], \mu_{dwP} [314]) = (0.0000028; 0.9999) = 0.0000028$$

**Fourth rule;** [R4] if  $\Delta\omega$  is Z and  $d\Delta\omega$  is N then  $i_q^* = x_4$ ; the operator used is AND, then:

$$\alpha_4 = \mu_{predikatR4} = \min(\mu_{wZ} [314], \mu_{dwN} [314]) = (0.6034; 0.0000030) = 0.0000030$$

**Fifth rule;** [R5] if  $\Delta\omega$  is Z and  $d\Delta\omega$  is Z then  $i_q^* = x_5$ ; the operator used is AND, then:

$$\alpha_5 = \mu_{predikatR5} = \min(\mu_{wZ} [314], \mu_{dwZ} [314]) = (0.6034; 0.6057) = 0.6034$$

**Sixth rule;** [R6] if  $\Delta\omega$  is Z and  $d\Delta\omega$  is P then  $i_q^* = x_6$ ; the operator used is AND, then:

$$\alpha_6 = \mu_{predikatR6} = \min(\mu_{wZ} [314], \mu_{dwP} [314]) = (0.6034; 0.9999) = 0.6034$$

**Seventh rule;** [R7] if  $\Delta\omega$  is P and  $d\Delta\omega$  is N then  $i_q^* = x_7$ ; the operator used is AND, then:

$$\alpha_7 = \mu_{predikatR7} = \min(\mu_{wP} [314], \mu_{dwN} [314]) = (0.9999; 0.0000030) = 0.0000030$$

**Eighth rule;** [R8] if  $\Delta\omega$  is P and  $d\Delta\omega$  is Z then  $i_q^* = x_8$ ; the operator used is AND, then:

$$\alpha_8 = \mu_{predikatR8} = \min(\mu_{wP} [314], \mu_{dwZ} [314]) = (0.9999; 0.6057) = 0.6057$$

**Ninth rule;** [R9] if  $\Delta\omega$  is P and  $d\Delta\omega$  is P then  $i_q^* = x_9$ ; the operator used is AND, then:

$$\alpha_9 = \mu_{predikatR9} = \min(\mu_{wP} [314], \mu_{dwP} [314]) = (0.9999; 0.9999) = 0.9999$$

### 1.3. Defuzzy

Defuzzy method used is a weighted average, obtained:

$$z = \frac{0.0000028.x_1 + 0.0000028.x_2 + 0.0000028.x_3 + \dots + 0.9999.x_9}{0.0000028 + 0.0000028 + 0.0000028 + \dots + 0.9999} = i_q^* \quad (25)$$

$$z = \frac{0.0000028.x_1 + 0.0000028.x_2 + 0.0000028.x_3 + \dots + 0.9999.x_9}{0.0000028 + 0.0000028 + 0.0000028 + \dots + 0.9999} = 1143.9$$

After we get the 1st equation, in the same way, then we take the second data for the second equation, and up to the ninth data for the ninth equation. We can summarize this analysis as:

#### 2. Data point $\Delta\omega = 313.91$ , $d\Delta\omega = -0.0087$ , and $i_q^* = 1347.4$

$$z = \frac{0.0000028.x_1 + 0.0000028.x_2 + 0.0000028.x_3 + \dots + 0.0000031.x_9}{0.0000028 + 0.0000028 + 0.0000028 + \dots + 0.0000031} = 1347.4 \quad (26)$$

#### 3. Data Point $\Delta\omega = 266.3$ , $d\Delta\omega = -0.0844$ , and $i_q^* = 2309.8$

$$z = \frac{0.0000037.x_1 + 0.0000037.x_2 + 0.0000031.x_3 + \dots + 0.0000031.x_9}{0.0000037 + 0.0000037 + 0.0000031 + \dots + 0.0000031} = 2309.8 \quad (27)$$

#### 4. Data point $\Delta\omega = 262.56$ , $d\Delta\omega = -0.0743$ , and $i_q^* = 2893.5$

$$z = \frac{0.0000052.x_1 + 0.0000052.x_2 + 0.0000031.x_3 + \dots + 0.0000031.x_9}{0.0000052 + 0.0000052 + 0.0000031 + \dots + 0.0000031} = 2892.5 \quad (28)$$

#### 5. Data point $\Delta\omega = 216.8$ , $d\Delta\omega = -0.0467$ , and $i_q^* = 3639.2$

$$z = \frac{0.00025.x_1 + 0.00025.x_2 + 0.0000029.x_3 + \dots + 0.0000029.x_9}{0.00025 + 0.00025 + 0.0000029 + \dots + 0.0000029} = 2892.5 \quad (29)$$

#### 6. Data point $\Delta\omega = 200.02$ , $d\Delta\omega = -0.1525$ , and $i_q^* = 4133.2$

$$z = \frac{0.00085.x_1 + 0.00085.x_2 + 0.0000028.x_3 + \dots + 0.0000028.x_9}{0.00085 + 0.00085 + 0.0000028 + \dots + 0.0000028} = 4133.2 \quad (30)$$

**7. Data point  $\Delta\omega = 135.05$ ,  $d\Delta\omega = -0.13$ , and  $i_q^* = 4877.4$** 

$$z = \frac{0.00397.x_1 + 0.0132x_2 + 0.0000028.x_3 + \dots + 0.0000028.x_9}{0.00085 + 0.00085 + 0.0000028 + \dots + 0.0000028} = 4877.4 \quad (31)$$

**8. Data point  $\Delta\omega = -0.825$ ,  $d\Delta\omega = -0.00014$ , and  $i_q^* = 5209.5$** 

$$z = \frac{0.9999.x_1 + 0.0133x_2 + 0.0000031.x_3 + \dots + 0.0000030.x_9}{0.9999 + 0.0133 + 0.0000031 + \dots + 0.0000030} = 5209.5 \quad (32)$$

**9. Data point  $\Delta\omega = 0.485$ ,  $d\Delta\omega = -0.00059$ , and  $i_q^* = 5213.4$** 

$$z = \frac{0.9997.x_1 + 0.0133x_2 + 0.0000031.x_3 + \dots + 0.0000031.x_9}{0.9997 + 0.0133 + 0.0000031 + \dots + 0.0000031} = 5213.4 \quad (33)$$

The nine equations above are then arranged into a matrix  $A.x = C$ , where:

$$A = \begin{bmatrix} 0.0000028 & 0.0000028 & 0.0000028 & 0.0000030 & 0.0132 & 0.0132 & 0.0000030 & 0.0132 & 0.9999 \\ 0.0000028 & 0.0000028 & 0.0000028 & 0.0132 & 0.0132 & 0.0000031 & 0.9999 & 0.0133 & 0.0000031 \\ 0.0000037 & 0.0000037 & 0.0000031 & 0.1221 & 0.0132 & 0.0000031 & 0.6719 & 0.0132 & 0.0000031 \\ 0.0000052 & 0.0000052 & 0.0000031 & 0.1396 & 0.0131 & 0.0000031 & 0.6287 & 0.0131 & 0.0000031 \\ 0.00025 & 0.00025 & 0.0000029 & 0.5296 & 0.0131 & 0.0000029 & 0.1907 & 0.0131 & 0.0000029 \\ 0.00085 & 0.00085 & 0.0000028 & 0.7184 & 0.0131 & 0.0000028 & 0.1024 & 0.0131 & 0.0000028 \\ 0.0397 & 0.0132 & 0.0000030 & 0.9221 & 0.0132 & 0.0000030 & 0.0037 & 0.0037 & 0.0000030 \\ 0.9999 & 0.0133 & 0.0000031 & 0.0132 & 0.0132 & 0.0000031 & 0.0000030 & 0.0000030 & 0.0000030 \\ 0.9997 & 0.0133 & 0.0000031 & 0.0141 & 0.0133 & 0.0000031 & 0.0000035 & 0.0000035 & 0.0000031 \end{bmatrix}$$

$$x = [x_1 \ x_2 \ x_3 \ x_4 \ x_5 \ x_6 \ x_7 \ x_8 \ x_9]^T$$

$$C = [1143.9 \ 1347.4 \ 2309.8 \ 2892.5 \ 3639.2 \ 4133.2 \ 4877.4 \ 5209.5 \ 5213.4]^T$$

$$A.x = C \Rightarrow x = A^{-1}.C;$$

$$x = [4.343e + 04 \ -5.978e + 05 \ -291.9 \ -7609 \ 2.027e + 05 \ 2039 \ 2.699e + 04 \ -4.028e + 05 \ 2.544e + 04]^T$$

$$x_1 = MF_1 = 4.343e + 04 \quad x_4 = MF_4 = -7609 \quad x_7 = MF_7 = 2.699e + 04$$

$$x_2 = MF_2 = -5.978e + 5 \quad x_5 = MF_5 = 2.027e + 05 \quad x_8 = MF_8 = -4.028e + 05$$

$$x_3 = MF_3 = -291.9 \quad x_6 = MF_6 = 2039 \quad x_9 = MF_9 = 2.544e + 04$$

**APPENDIX. B**

To initialize the simulation model, a three-phase induction motor is used following the following specifications:

Power motor : 5 Hp; terminal voltage: 220 Volt; number of poles: 4; frequency: 60 Hz

Dc current test,  $V_{dc} = 13.8$  Volt;  $I_{dc} = 13.0$  Amp.

Blocked Rotor Test,  $V_{br} = 23.5$  Volt;  $I_{br} = 12.9$  Amp;  $P_{br} = 469$  Watt;  $f = 15$  hz; Slip =  $S = 5.3\% = 0.053$ .

After carrying out calculations to determine the characteristics of the induction motor, it is obtained

$$r_s = 0.5308 \ \Omega; r'_r = 0.4146 \ \Omega; X_{ls} = 0.2365 \ \Omega; X'_{lr} = 0.2365 \ \Omega; X_M = 32.3639 \ \Omega$$

**NOMENCLATURE**

$r_s$	stator resistance	$H$	inertia constant
$r'_r$	rotor resistance	$i_{ds}, v_{ds}$	stator d-axis current dan voltage
$T_e$	torque electromagnetic	$i_{dr}, v_{dr}$	rotor d-axis current dan voltage
$T_L$	load torque	$i_{qs}, v_{qs}$	stator q-axis current dan voltage
$X_{ls}$	stator leakage reactance	$i_{qr}, v_{qr}$	rotor q-axis current dan voltage
$X'_{lr}$	rotor leakage reactance	$J$	inertia of motor
$X_M$	magnetizing reactance	$L_{ls}$	stator self inductance
$\lambda, \psi$	flux linkage	$L'_{lr}$	rotor self inductance
$\omega_b$	nominal speed rad/sec	$L_M$	mutual inductance
$\omega_r$	rotor speed rad/sec	$P$	number of poles

## REFERENCES

- [1] S. Oktavia, L. Dwiridal, N. Y. Sudiar, "Analysis of Surface Wind Speed at Minangkabau International Airport for the period 2011-2020 using the Windrose Method," In *Journal of Physics: Conference Series*, vol. 2582, no. 1, p. 012006, 2023, <https://doi.org/10.1088/1742-6596/2582/1/012006>.
- [2] M. Marghany, *Synthetic aperture radar imaging mechanism for oil spills*. Gulf Professional Publishing, 2019, <https://doi.org/10.1016/B978-0-12-818111-9.00007-0>.
- [3] S. Rafa *et al.*, "Implementation of a new fuzzy vector control of induction motor," *ISA transactions*, vol. 53, no. 3, pp. 744-754, 2014, <https://doi.org/10.1016/j.isatra.2014.02.005>.
- [4] A. M. Hannan *et al.*, "A quantum lightning search algorithm-based fuzzy speed controller for induction motor drive," *IEEE Access*, vol. 6, pp. 1214-1223, 2017, <https://doi.org/10.1109/ACCESS.2017.2778081>.
- [5] M. A. Hannan *et al.*, "Quantum-behaved lightning search algorithm to improve indirect field-oriented Fuzzy-PI control for IM drive," *IEEE Transactions on Industry Applications*, vol. 54, no. 4, pp. 3793-3805, 2018, <https://doi.org/10.1109/TIA.2018.2821644>.
- [6] N. Farah *et al.*, "A novel self-tuning fuzzy logic controller based induction motor drive system: An experimental approach," *IEEE Access*, vol. 7, pp. 68172-68184, 2019, <https://doi.org/10.1109/ACCESS.2019.2916087>.
- [7] N. Farah *et al.*, "Investigation of the computational burden effects of self-tuning fuzzy logic speed controller of induction motor drives with different rules sizes," *IEEE Access*, vol. 9, pp. 155443-155456, 2021, <https://doi.org/10.1109/ACCESS.2021.3128351>.
- [8] Q. A. Tarbosh *et al.*, "Review and investigation of simplified rules fuzzy logic speed controller of high performance induction motor drives," *IEEE Access*, vol. 8, pp. 49377-49394, 2020, <https://doi.org/10.1109/ACCESS.2020.2977115>.
- [9] Z. M. Elbarbary, H. A. Hamed, E. E. El-Kholy, "Comments on "A performance investigation of a four-switch three-phase inverter-fed IM drives at low speeds using fuzzy logic and PI controllers,"" *IEEE Transactions on Power Electronics*, vol. 33, no. 9, pp. 8187-8188, 2017, <https://doi.org/10.1109/TPEL.2017.2743681>.
- [10] Y. Liyong, L. Yinghong, C. Yaai, L. Zhengxi, "A novel fuzzy logic controller for indirect vector control induction motor drive," *IEEE World Congress on Intelligent Control and Automation*, vol. 7, pp. 24-28, 2008, <https://doi.org/10.1109/WCICA.2008.4592897>.
- [11] V. Bindu, A. Unnikrishnan, R. Gopikakumari, "Fuzzy logic based sensorless vector control of Induction motor," In *2012 Annual IEEE India Conference (INDICON)*, pp. 514-518, 2012, <https://doi.org/10.1109/INDCON.2012.6420672>.
- [12] A. B. Debbagh, M. Bendjebbar, M. Benslimanem, M. Zerikat, "Sensorless Fuzzy logic Control applied on induction motor in real-time," *IEEE International Conference on Advanced Electrical Engineering (ICAEE)*, pp. 1-6, 2019, <https://doi.org/10.1109/ICAEE47123.2019.9014801>.
- [13] V. S. Virkar, S. S. Karvekar, "Luenberger observer based sensorless speed control of induction motor with Fuzzy tuned PID controller," *IEEE International Conference on Communication and Electronics Systems (ICCES)*, pp. 503-508, 2019, <https://doi.org/10.1109/ICCES45898.2019.9002268>.
- [14] B. Sahu, K. B. Mohanty, S. Pati, "A comparative study on fuzzy and PI speed controllers for field-oriented induction motor drive," *IEEE Modern Electric Power Systems*, pp. 1-7, 2010, <https://doi.org/10.1109/IECR.2010.5720134>.
- [15] M. D. Pop, D. Pescaru, M. V. Micea, "Mamdani vs. Takagi-Sugeno Fuzzy Inference Systems in the Calibration of Continuous-Time Car-Following Models," *Sensors*, vol. 23, no. 21, 8791, 2023 <https://doi.org/10.3390/s23218791>
- [16] N. Tri, N. N. Khoat, "Research on a Sugeno Fuzzy Logic Controller Compared to a Mamdani-Based PI-Type Fuzzy Logic Inference Model," *Tạp chí Khoa học và Công nghệ-Đại học Đà Nẵng*, vol. 20, no. 2, pp. 57-62, 2022, <https://doi.org/10.31130/ud-jst.2022.177ICT>.
- [17] P. Setiawan, "Improvement of Electrical Power System Dynamic Stability Using Fuzzy Logic," In *Seminar Nasional Teknologi Informasi dan Kedirgantaraan (SENATIK)* Sekolah Tinggi Teknologi Adisutjipto Yogyakarta, vol. 4, pp. 303-312, 2018, <http://dx.doi.org/10.28989/senatik.v4i0.149>.
- [18] R. Raj, B. M. Mohan, "General structure of interval type-2 fuzzy PI/PD controller of Takagi-Sugeno type," *Engineering Applications of Artificial Intelligence*, vol. 87, 103273, pp. 1-13, 2020, <https://doi.org/10.1016/j.engappai.2019.103273>.
- [19] P. C. Krause, O. Wasynczuk, S. D. Sudhoff, S. Pekarek, "Analysis of electric machinery and drive systems," *IEEE press*, vol. 2, 2002, <https://doi.org/10.1002/9783527679065>.
- [20] G. I. Orfanoudakis, M. A. Yuratich, S. M. Sharkh, "Current balancing of scalar-controlled induction motors with long imbalanced cables for artificial lift systems," *e-Prime-Advances in Electrical Engineering, Electronics and Energy*, vol. 7, 100391, pp. 1-10, 2024, <https://doi.org/10.1016/j.prime.2023.100391>.
- [21] M. P. Sruthi, C. Nagamani, G. S. Ilango, "An improved algorithm for direct computation of optimal voltage and frequency for induction motors," *Engineering science and technology, an international journal*, vol. 20, no. 5, pp. 1439-1449, 2017, <https://doi.org/10.1016/j.jestch.2017.11.007>.
- [22] Y. Wang, H. H. Eldeeb, H. Zhao, O. A. Mohammed, "Sectional variable frequency and voltage regulation control strategy for energy saving in beam pumping motor systems," *IEEE Access*, vol. 7, pp. 92456-92464, 2019, <https://doi.org/10.1109/ACCESS.2019.2927525>.
- [23] N. A. J. Salih, H. T. R. Altaie, W. K. Al-Azzawi, M. J. Mnati, "Design and implementation of a driver circuit for three-phase induction motor based on STM32F103C8T6," *Bulletin of Electrical Engineering and Informatics*, vol. 12, no. 1, pp. 42-50, 2023, <https://doi.org/10.11591/eei.v12i1.4276>.

- [24] K. A. M. Annuar *et al.*, "Squirrel cage induction motor scalar control constant V/F analysis," *TELKOMNIKA (Telecommunication Computing Electronics and Control)*, vol. 17, no. 1, pp. 417-424, 2019, <http://doi.org/10.12928/telkomnika.v17i1.8818>.
- [25] H. S. Dakheel, Z. B. Abdulla, H. J. Jawad, A. J. Mohammed, "Comparative analysis of PID and neural network controllers for improving starting torque of wound rotor induction motor," *TELKOMNIKA (Telecommunication Computing Electronics and Control)*, vol. 18, no. 6, pp. 3142-3154, 2020, <http://doi.org/10.12928/telkomnika.v18i6.14571>.
- [26] R. Singh, S. K. Bajpai, H. S. Sandhu, "Comparative study of PWM control and PI control of Induction motor," *Bulletin of Electrical Engineering and Informatics*, vol. 4, no. 1, pp. 53-58, 2015, <https://doi.org/10.11591/eei.v4i1.322>.
- [27] G. Kohlrusz, D. Fodor, "Comparison of scalar and vector control strategies of induction motors," *Hungarian Journal of Industry and Chemistry*, vol. 39, no. 2, pp. 265-270, 2011, <https://doi.org/10.1515/422>.
- [28] H. A. Toliyat, S. G. Campbell, "DSP-based electromechanical motion control," *CRC press*, 2003, <https://uodiyala.edu.iq/uploads/PDF%20ELIBRARY%20UODIYALA/EL47/DSP-Based%20Electromechanical%20Motion%20Control.pdf>.
- [29] D. W. Hart, D. W. Hart, "Power electronics," *McGraw-Hill*, vol. 166, 2011, [https://www.ece.ufl.edu/wp-content/uploads/syllabi/Fall2018/EEE5317C\\_F\\_2018.pdf](https://www.ece.ufl.edu/wp-content/uploads/syllabi/Fall2018/EEE5317C_F_2018.pdf).
- [30] J. Holtz, "Pulsewidth modulation-a survey," *IEEE transactions on Industrial Electronics*, 39(5), 410-420, 1992. <https://doi.org/10.1109/41.161472>.
- [31] R. Krishnan, "Electric motor drives: modeling, analysis and control," *Prentice Hall*, 2001, <https://cir.nii.ac.jp/crid/1130282272968928512>.
- [32] P. Setiawan *et al.*, "Study of Permanent Magnet Synchronous Motor With LQG Controller and Observer On The Hydraulic Pump System," *Jurnal EECIS (Electrics, Electronics, Communications, Controls, Informatics, Systems)*, vol. 17, no. 2, pp. 41-52, 2023, <https://doi.org/10.21776/jeeccis.v17i2.1637>.
- [33] L. Struharňanský, J. Vittek, P. Makyš, J. Ilončíak, "Vector control techniques for traction drive with induction machines-comparison," *Procedia engineering*, vol. 192, pp. 851-856, 2017, <https://doi.org/10.1016/j.proeng.2017.06.147>.
- [34] H. H. Vo *et al.*, "Pulse-width modulation direct torque control induction motor drive with Kalman filter," *TELKOMNIKA (Telecommunication Computing Electronics and Control)*, vol. 19, no. 1, pp. 277-284, 2021, <http://doi.org/10.12928/telkomnika.v19i1.16247>.
- [35] Y. N. I. Alothman, W. E. A. -Lateef, S. A. H. Gitaffa, "Using sensorless direct torque with fuzzy proportional-integral controller to control three phase induction motor," *Bulletin of Electrical Engineering and Informatics*, vol. 12, no. 2, pp. 738-748, 2023, <https://doi.org/10.11591/eei.v12i2.3991>.
- [36] A. Berzoy, J. Rengifo, O. Mohammed, "Fuzzy predictive DTC of induction machines with reduced torque ripple and high-performance operation," *IEEE Transactions on Power Electronics*, vol. 33, no. 3, pp. 2580-2587, 2017, <https://doi.org/10.1109/TPEL.2017.2690405>.
- [37] K. Bouhoune, K. Yazid, M. S. Boucherit, M. Mena, "Fuzzy logic-based direct torque control for induction machine drive," *IEEE Mediterranean Conference on Control and Automation (MED)*, vol. 25, pp. 577-582, 2017, <https://doi.org/10.1109/MED.2017.7984179>.
- [38] A. Ammar *et al.*, "Predictive direct torque control with reduced ripples and fuzzy logic speed controller for induction motor drive," *IEEE International Conference on Electrical Engineering-Boumerdes (ICEE-B)* vol. 5, pp. 1-6, 2017, <https://doi.org/10.1109/ICEE-B.2017.8191978>.
- [39] A. A. Adam, Y. Haroen, A. Purwadi, A. S. Rohman, "A study of a three phase induction motor performances controlled by indirect vector and predictive torque control," *IEEE International Conference on Electric Vehicular Technology (ICEVT)*, vol. 5, pp. 204-209, 2018, <https://doi.org/10.1109/ICEVT.2018.8628372>.
- [40] F. Wang *et al.*, "Advanced control strategies of induction machine: Field oriented control, direct torque control and model predictive control," *Energies*, vol. 11, no. 120, pp.1-13, 2018, <https://doi.org/10.3390/en11010120>.
- [41] K. Rahman *et al.*, "Field-oriented control of five-phase induction motor fed from space vector modulated matrix converter," *IEEE Access*, vol. 10, pp. 17996-18007, 2022, <https://doi.org/10.1109/ACCESS.2022.3142014>.
- [42] I. M. Mehedi *et al.*, "Simulation analysis and experimental evaluation of improved field-oriented controlled induction motors incorporating intelligent controllers," *IEEE Access*, vol. 10, pp. 18380-18394, 2022, <https://doi.org/10.1109/ACCESS.2022.3150360>.
- [43] F. Zhao *et al.*, "The Effects of Parameter Variations on the Torque Control of Induction Motor," *IEEE CAA International Conference on Vehicular Control and Intelligence (CVCI)*, vol. 4, pp. 757-760, 2020, <https://doi.org/10.1109/CVCI51460.2020.9338443>.
- [44] N. Nazeer, T. N. Shahina, "Speed Control For Indirect Vector Control Of Induction Motor Drives At Low Speeds," *IEEE International Conference on Intelligent Computing, Instrumentation and Control Technologies (ICICT)*, vol. 1, pp. 1111-1118, 2019, <https://doi.org/10.1109/ICICT46008.2019.8993223>.
- [45] I. Ferdiansyah, M. R. Rusli, B. Praharsena, H. Toar, E. Purwanto, "Speed control of three phase induction motor using indirect field oriented control based on real-time control system," *IEEE International Conference on Information Technology and Electrical Engineering (ICITEE)*, vol. 10, pp. 438-442, 2018, <https://doi.org/10.1109/ICITEE.2018.8534864>.

- [46] S. Shukla, B. Singh, "Reduced current sensor based solar PV fed motion sensorless induction motor drive for water pumping," *IEEE Transactions on Industrial Informatics*, vol. 15, no. 7, pp. 3973-3986, 2018, <https://doi.org/10.1109/TII.2018.2885795>.
- [47] J. R. Dominguez, I. Duenas, S. O. Cisneros, "Discrete-time modeling and control based on field orientation for induction motors," *IEEE Transactions on Power Electronics*, vol. 35, no. 8, pp. 8779-8793, 2020, <https://doi.org/10.1109/TPEL.2020.2965632>.
- [48] D. Zellouma, Y. Bekakra, H. Benbouhenni, "Field-oriented control based on parallel proportional–integral controllers of induction motor drive," *Energy Reports*, vol. 9, pp. 4846-4860, 2023, <https://doi.org/10.1016/j.egy.2023.04.008>.
- [49] T. D. Do, N. D. Le, V. H. Phuong, N. T. Lam, "Implementation of FOC algorithm using FPGA for GaN-based three phase induction motor drive," *Bulletin of Electrical Engineering and Informatics*, vol. 11, no. 2, pp. 636-645, 2022, <https://doi.org/10.11591/eei.v11i2.3569>.
- [50] R. Rahmatullah, A. Ak, N. F. O. Serteller, "Design of Sliding Mode Control using SVPWM Modulation Method for Speed Control of Induction Motor," *Transportation Research Procedia*, vol. 70, pp. 226-233, 2023, <https://doi.org/10.1016/j.trpro.2023.11.023>.
- [51] H. R. Khoei, M. Zolfaghari, "New model reference adaptive system speed observer for field-oriented control induction motor drives using neural networks," *Bulletin of Electrical Engineering and Informatics*, vol. 5, no. 1, pp. 25-36, 2016, <https://doi.org/10.11591/eei.v5i1.520>.
- [52] S. Hesari, M. Noruziazghandi, A. A. Shojaei, M. Neyestani, "Investigating the intelligent methods of loss minimization in induction motors," *Telkomnika (Telecommunication Computing Electronics and Control)*, vol. 16, no. 3, pp. 1034-1053, 2018, <http://doi.org/10.12928/telkomnika.v16i3.8293>.
- [53] T. C. Tran *et al.*, "Comparison of the speedy estimate methods of the induction motors," *TELKOMNIKA (Telecommunication Computing Electronics and Control)*, vol. 21, no. 1, pp. 223-234, 2022, <http://doi.org/10.12928/telkomnika.v21i1.24089>.
- [54] M. H. Basappa, P. Viswanathan, "Various control methods of permanent magnet synchronous motor drives in electric vehicle: a technical review," *TELKOMNIKA (Telecommunication Computing Electronics and Control)*, vol. 20, no. 6, pp. 1225-1229, 2022, <http://doi.org/10.12928/telkomnika.v20i6.24236>.
- [55] M. Barfi *et al.*, "Improving robotic hand control via adaptive Fuzzy-PI controller using classification of EMG signals," *Heliyon*, vol. 8, no. 12, 2022, <https://doi.org/10.1016/j.heliyon.2022.e11931>.
- [56] J. Benić, A. Pender, J. Kasać, T. Stipančić, "Sugeno-Type Fuzzy Ontology PI Controller for Proportional Electrohydraulic System," *IFAC-Papers OnLine*, vol. 56, no. 2, pp. 8732-8737, 2023, <https://doi.org/10.1016/j.ifacol.2023.10.056>.
- [57] T. Pidikiti, B. Gireesha, M. Subbarao, V. M. Krishna, "Design and control of Takagi-Sugeno-Kang fuzzy based inverter for power quality improvement in grid-tied PV systems," *Measurement: Sensors*, vol. 25, no. 100638, pp. 1-7, 2023, <https://doi.org/10.1016/j.measen.2022.100638>.

## BIOGRAPHY OF AUTHORS



**Paulus Setiawan**, earned his Bachelor of Electrical Engineering in 2000 from Trisakti University and a Master of Electrical Engineering degree in 2004 from Gadjah Mada University. He is currently serving as a full-time lecturer in Electrical Engineering at the Institut Teknologi Dirgantara Adisutjipto Yogyakarta. His research interests are in the area of control systems, electric machines and drives. He can be contacted at e-mail: [paulussetiawan@itda.ac.id](mailto:paulussetiawan@itda.ac.id). Orcid-id: <https://orcid.org/0000-0002-2655-2781>.



**Muchamand Wizdan Dharmawan**, is a College Students who are currently undergoing education in the study program of electrical engineering at the Faculty of Industrial Technology at the Institut Teknologi Dirgantara Adisutjipto Yogyakarta with a bachelor's degree. He can be contacted at e-mail: [mwizdandarmawan@gmail.com](mailto:mwizdandarmawan@gmail.com).



**Prasadanto Nur Santoso**, earned his Bachelor of Industrial Engineering in 2005 from UPN "Veteran" Yogyakarta and a Master of Science degree in 2017 from Universitas Gadjah Mada. He is currently serving as a full-time lecturer in Industrial Engineering Departement at the Institut Teknologi Dirgantara Adisutjipto Yogyakarta. He can be contacted at e-mail: [industri.pras@itda.ac.id](mailto:industri.pras@itda.ac.id). Orcid-id: <https://orcid.org/0000-0001-9111-7228>.



**Elisabeth Anna Pratiwi**, graduated with Bachelor of Engineering at STT Adisutjipto in 2018 and graduated with Master of Science at National Cheng Kung University, Taiwan, in 2021. Currently, she is a lecturer in Aerospace Engineering in Institut Teknologi Dirgantara Adisutjipto Yogyakarta. She has research interest in field of heat-transfer combustion in aerospace. She can be contacted at e-mail: [anna@itda.ac.id](mailto:anna@itda.ac.id). Orcid-id: <https://orcid.org/0000-0002-6218-4824>.



**Okto Dinaryanto**, earned his Doctoral of Mechanical Engineering in 2018 from Gadjah Mada University. He is currently serving as a full-time lecturer in Mechanical Engineering at the Institut Teknologi Dirgantara Adisutjipto Yogyakarta. His research interests are in the area of Fluid Mechanics, Signal Processing and Numeric Analysis. He can be contacted at e-mail: [okto.dinaryanto@itda.ac.id](mailto:okto.dinaryanto@itda.ac.id). Orcid-id: <https://orcid.org/0000-0002-9598-6970>.